POWER ELECTRONICS AND DRIVES
Vol. 1(36), No. 2, 2016 DOI: 10.5277/PED160207

STABILITY ANALYSIS OF MRASS^{CC} SPEED ESTIMATOR IN MOTORING AND REGENERATING MODE*

MATEUSZ KORZONEK, TERESA ORŁOWSKA-KOWALSKA

Wrocław University of Science and Technology, Wybrzeże Wyspiańskiego 27, 50-370 Wrocław, Poland,
phone: +48 (71) 320 37 16, +48 (71) 320 26 40,
e-mail: mateusz.korzonek@pwr.edu.pl; teresa.orlowska-kowalska@pwr.edu.pl

Abstract: This paper deals with the stability analysis of MRAS current speed estimator in a motoring and regenerating mode. The unstable operating points of the estimator, mainly in a regenerating mode are widely discussed. The expanded version of the estimator MRAS^{CC} is proposed to provide its stability in the whole operating range. The new correction coefficients for two analyzed stabilization methods are proposed. Finally, simulation results confirming the theoretical analysis are presented

Keywords: *Induction motor, vector control, MRAS-type estimator, stability, regenerating mode, stabilization methods*

1. INTRODUCTION

Electric drives with induction motors using vector control methods are now widely used in industrial practice. In these systems, the implementation of field-oriented control (FOC) or direct torque control (DTC) algorithms require the state variable estimators, such as the rotor or stator fluxes [1]. In some applications also the speed sensorless induction motor drives are the subject of interest [2], [3]. The advantages of sensorless systems are: saving space allocated to drive, lower costs, fewer cables, higher reliability. Although many methods of estimating the angular velocity of the induction motor have been developed, these issues are still analyzed and published in the literature.

A broad overview of these methods was included, among others, in [2], [3]. These methods can be divided into 3 main groups (Fig. 1). The first one includes physical methods, which take advantage of phenomena taking place in the machine. The next methods are neural methods that use artificial intelligence (artificial neural networks, including neuro-fuzzy structures). The third one, the most developed and studied group comprises algorithmic methods. They are based on mathematical models of the

* Manuscript received: July 14, 2016; accepted: August 8, 2016.

induction motor and the different methods of control theory. This group can be divided into more parts – estimators, state variables observers, and Kalman filters.

Among the state variable observers we can distinguish a nonlinear observer, an extended observer, observers which use sliding mode theory (Sliding Mode Observer – SMO [4], Dual-Mode – DM [5]) and the most popular of them – Adaptive Full-Order Observer (AFO) [6]. In the case of AFO, many articles have been published, in which appropriate selection of gain matrix or adaptation mechanism was proposed, to improve observer stability especially in the regenerating mode [7]–[13].

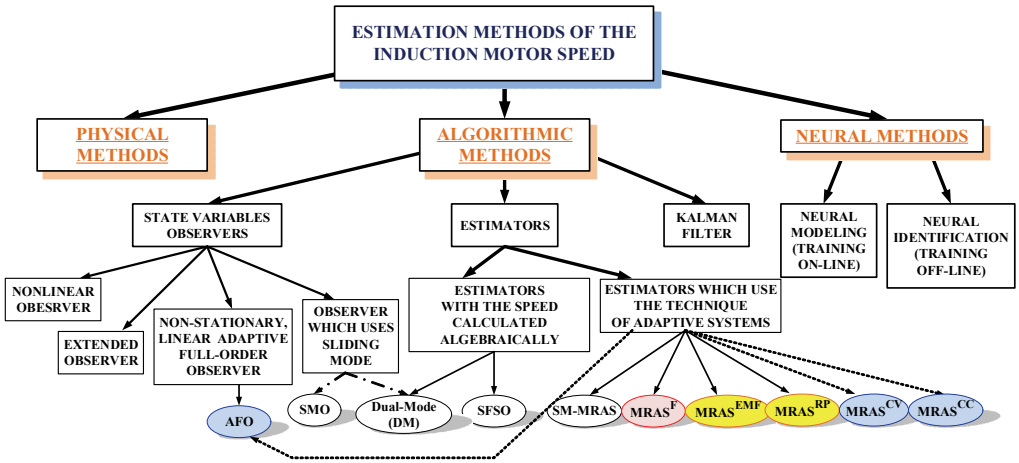

Fig. 1. Estimation methods of the induction motor speed

State estimators can be divided into two groups. The estimators with the rotor speed value calculated algebraically, based on the estimated rotor flux vector angular speed and calculated rotor slip pulsation, belong to the first group. Examples of such estimators have been proposed in [3], [14]–[16].

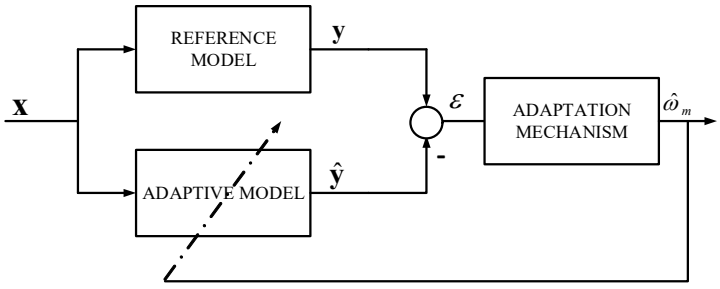

Fig. 2. The basic block scheme of MRAS type estimators

The second group consists of estimators which use a technique of adaptive systems – MRAS-type speed estimators. The basic structure of the MRAS-type estimator consists of three blocks: a reference model, an adaptive model and an adaptation mechanism (usually it is PI controller) (Fig. 2).

Estimators of this group can be divided into next three groups according to the error signal which is used in the speed adaptation mechanism:

- the error in the form of a vector product of the rotor flux vectors estimated from the voltage and current rotor flux simulators – MRAS^{F} [17], [18]; it is one of the most popular MRAS speed estimators;
- the error in the form of a vector product of the estimated values of electromotive force MRAS^{EMF} [19] and extension of this estimator, where the error is in the form of the difference between the reactive power values (the vector product of the electromotive force and the stator current) estimated by the reference and adaptive models – MRAS^{RP} [20];
- the error in the form of vector product of the estimated rotor flux vector and the stator current error (between measured and estimated current vectors) – MRAS^{CV} [21] and MRAS^{CC} [22].

In recent years, some research has been published concerning modified MRAS-type estimator, with sliding mode controller instead of the PI controller in the speed adaptation loop – SM-MRAS [23].

The third approach is unconventional, since the induction motor is considered as a reference model in the case of these current-based MRAS-type estimators. Also the speed adaptation mechanism is the same as in case of the adaptive full-order observer AFO [6]. The above two features involve the possibility of classifying both AFO and MRAS^{CC_CV} into one group. It should be mentioned that the influence of the induction motor parameter changes to performance of each estimator of this group was examined in [14], from the point of view of the speed estimation quality and stability in the motoring mode. In the case of MRAS^{CC} the first study of its stability in the regenerating mode was made in [24] and some solutions for estimator stabilization were proposed.

In this paper, a detailed stability analysis of the MRAS^{CC} speed estimator in the regenerating operation mode is presented as well as new solution for the estimator stabilization is proposed. The paper is divided into several sections. After the discussion of the state variable estimation methods, with emphasis given to the MRAS-type techniques in the Introduction part, the mathematical models of the induction motor and analysed MRAS^{CC} estimator are shown in Section 2. In Section 3, a detailed stability analysis of the estimator is presented. Next, methods for correcting the stability range in regenerating mode are discussed. In Section 5, the simulation results of testing the MRAS^{CC} estimator in motoring and regenerating modes, for the induction motor drive with direct field-oriented control are presented. The paper is concluded with summary of the results obtained.

2. MATHEMATICAL MODELS USED FOR STABILITY ANALYSIS

2.1. MATHEMATICAL MODEL OF AN INDUCTION MOTOR

In this research, a mathematical model of induction motor was used, which was represented in spatial vector notation, using commonly applied simplifying assumptions and was written in coordinate system rotating synchronously with the rotor flux, in relative units [3]. The state equation for the electromagnetic part of the induction motor takes the following form

$$\begin{aligned} T_N \frac{d\mathbf{x}}{dt} &= \mathbf{A}(\omega_m)\mathbf{x} + \mathbf{B}\mathbf{u}, \\ \mathbf{y} &= \mathbf{C}\mathbf{x}, \end{aligned} \tag{1}$$

where $\mathbf{x} = \begin{bmatrix} \mathbf{i}_s \\ \boldsymbol{\psi}_r \end{bmatrix}$, $\mathbf{y} = \mathbf{i}_s$, $\mathbf{C} = [1\ 0]$, and $\mathbf{i_s} = i_{sx} + ji_{sy}$, $\mathbf{u_s} = u_{sx} + ju_{sy}$, $\boldsymbol{\Psi}_\mathbf{r} = \Psi_{rx} + j\Psi_{ry}$, ω_m – rotor angular speed.

By substituting the parameters of the induction motor and using complex notation the following equation is obtained

$$T_N \frac{d}{dt}\begin{bmatrix} \mathbf{i}_s \\ \boldsymbol{\psi}_r \end{bmatrix} = \begin{bmatrix} -\dfrac{r_1}{l_\sigma} - j\omega_s & \left(\dfrac{k_r}{l_\sigma \tau_r} - j\dfrac{k_r}{l_\sigma}\omega_m\right) \\ r_r k_r & \left(-\dfrac{1}{\tau_r} - j(\omega_s - \omega_m)\right) \end{bmatrix} \begin{bmatrix} \mathbf{i}_s \\ \boldsymbol{\psi}_r \end{bmatrix} + \begin{bmatrix} \dfrac{1}{l_\sigma} \\ 0 \end{bmatrix} \mathbf{u}_s, \tag{2}$$

where r_s, r_r – stator and rotor resistance, l_s, l_r, l_m – stator and rotor leakage inductance, magnetizing inductance, σ – total leakage factor, ω_s – stator frequency, $\omega_s - \omega_m = \omega_r$ – rotor frequency in [p.u.] (or slip frequency), f_{sN} – stator nominal frequency, $k_r = \dfrac{l_m}{l_r}$, $l_\sigma = \sigma l_s$, $r_1 = r_s + r_r k_r^2$, $\tau_r = l_r / r_r$, $T_N = 1/2\pi f_{sN}$.

2.2. MATHEMATICAL MODEL OF THE CURRENT SPEED ESTIMATOR – MRAS^{CC}

The current speed estimator MRAS^{CC}, which was proposed in [22], is presented in Fig. 3. The scheme includes a model of stator current estimator

$$T_N \frac{d}{dt}\hat{\mathbf{i}}_s = \frac{1}{l_\sigma}\mathbf{u}_s - \left(\frac{r_1}{l_\sigma} + j\omega_s\right)\hat{\mathbf{i}}_s + \left(\frac{k_r}{l_\sigma \tau_r} - j\frac{k_r}{l_\sigma}\hat{\omega}_m\right)\hat{\boldsymbol{\psi}}_r. \tag{3}$$

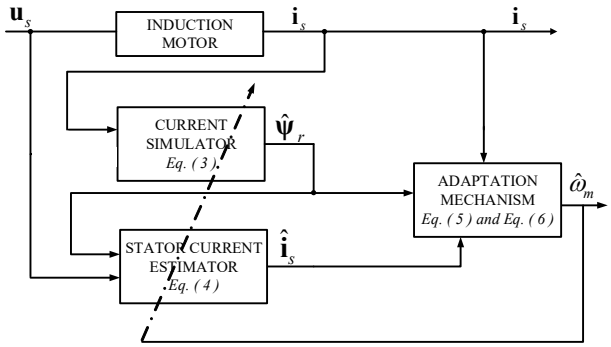

Fig. 3. A block diagram of the basic MRAS^{CC}

This model requires information about rotor flux, which is obtained from the classical current simulator [3]

$$T_N \frac{d}{dt}\hat{\boldsymbol{\psi}}_r = \left[k_r r_r \mathbf{i}_s - \left(\frac{1}{\tau_r} + j\left(\omega_s - \hat{\omega}_m\right) \right) \hat{\boldsymbol{\psi}}_r \right]. \tag{4}$$

Both models are tuneable by estimated rotor speed, which is calculated in the adaptation mechanism

$$\frac{d}{dt}\hat{\omega}_m = K_i \varepsilon + K_p \frac{d}{dt}\varepsilon\,, \tag{5}$$

where input error of the PI controller, compared to original solution [22], is modified according to the proposal presented firstly in [10]

$$\varepsilon = \Im\{\underline{e}_i \underline{\hat{\boldsymbol{\psi}}}_R^*\} = \Im\{(e_{ix} + je_{iy})(\hat{\psi}_{rx} - j\hat{\psi}_{ry})\} = \hat{\psi}_{rx} e_{iy} - \hat{\psi}_{ry} e_{ix}\,, \tag{6}$$

where $\mathbf{e}_i = \mathbf{i}_s - \hat{\mathbf{i}}_s$ is the estimation error of the stator current vector.

The block diagram of this speed estimator is presented in Fig. 3.

The mathematical model of the current speed estimator MRAS^{CC} can be written in the form similar to AFO [6], [9]–[13], through the expansion of its basic version by the gain matrix **G**. Equations (3) and (4) are now represented by the following state equation

$$\begin{aligned} T_N \frac{d\hat{\mathbf{x}}}{dt} &= \hat{\mathbf{A}}^e(\omega_m)\hat{\mathbf{x}} + \mathbf{B}\mathbf{u} + \mathbf{K}\mathbf{y} + \mathbf{G}\mathbf{e}_i, \\ \hat{\mathbf{y}} &= \mathbf{C}\hat{\mathbf{x}}\,, \end{aligned} \tag{7}$$

where **K** – matrix resulting directly from (4), which depends on motor parameters multiplied next by the measured stator current (not estimated current like in AFO) – see (8).

By substituting the parameters of the induction motor into state, control and **K** matrices, the following state equation of the estimator is obtained, with additional modification of its structure like in [24]

$$T_N \frac{d}{dt}\begin{bmatrix}\hat{\mathbf{i}}_s\\ \hat{\boldsymbol{\psi}}_r\end{bmatrix} = \begin{bmatrix} -\frac{r_1}{l_\sigma} - j\omega_s & \frac{k_r}{l_\sigma \tau_r} - j\frac{k_r}{l_\sigma}\hat{\omega}_m \\ 0 & -\frac{1}{\tau_r} - j(\omega_s - \hat{\omega}_m) \end{bmatrix} \begin{bmatrix}\hat{\mathbf{i}}_s\\ \hat{\boldsymbol{\psi}}_r\end{bmatrix} + \begin{bmatrix}\frac{1}{l_\sigma}\\ 0\end{bmatrix} \mathbf{u}_s + \begin{bmatrix}0\\ r_r k_r\end{bmatrix} \mathbf{y} + \begin{bmatrix}\mathbf{g}_s\\ \mathbf{g}_r\end{bmatrix} \mathbf{e}_i, \quad (8a)$$

$$\hat{\mathbf{y}} = \begin{bmatrix}1 & 0\end{bmatrix} \begin{bmatrix}\hat{\mathbf{i}}_s\\ \hat{\boldsymbol{\psi}}_r\end{bmatrix}, \quad (8b)$$

where $\mathbf{g}_s = g_{sx} + jg_{sy}$; $\mathbf{g}_r = g_{rx} + jg_{ry}$.

Additionally, the input error of the PI controller, compared to the original solution [22], can be modified according to the proposal presented firstly in [10]

$$\varepsilon' = \Im\{e^{-j\varphi}\underline{e}_i \underline{\hat{\boldsymbol{\psi}}}_R^*\} = \Im\{(\cos\varphi - j\sin\varphi)(e_{ix} + je_{iy})(\hat{\psi}_{rx} - j\hat{\psi}_{ry})\}$$
$$= \hat{\psi}_{rx}e_{iy}\cos\varphi - \hat{\psi}_{rx}e_{ix}\sin\varphi - \hat{\psi}_{ry}e_{ix}\cos\varphi - \hat{\psi}_{ry}e_{ix}\sin\varphi. \quad (9)$$

Thus the modified speed adaptation algorithm with the additional correction of current error will take the following form

$$\frac{d}{dt}\hat{\omega}_m = -K_i\varepsilon' - K_p\frac{d}{dt}\varepsilon'. \quad (10)$$

The new form of this estimator is illustrated in a block diagram in Fig. 4.

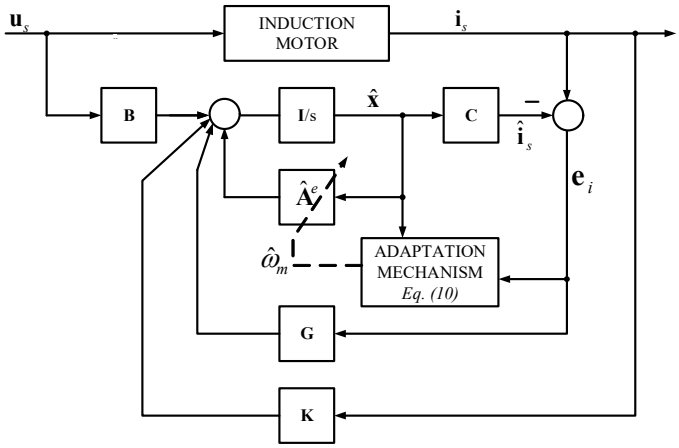

Fig. 4. A block diagram of the modified MRAS^{CC} estimator

3. STABILITY ANALYSIS OF MRAS^{CC} ESTIMATOR

3.1. METHODOLOGY OF THE ESTIMATOR STABILITY ANALYSIS

The algorithm of the estimator stability analysis can be described in a few steps:

(1) Formulation of the state estimation error equation for the full model of the estimator

The state vector of estimator (8), consisting of two electromagnetic state variables (estimated stator current and rotor flux vectors) is extended by the estimated angular velocity of the induction motor and thus the nonlinear state equation of the estimator is obtained. By subtracting the combined equations of the estimator (8) and (10) from state equation of the induction motor model (2), the state estimation error equation is obtained, where the error state vector is defined as follows

$$\mathbf{e} = \begin{bmatrix} \mathbf{e}_i \\ \mathbf{e}_\psi \\ \mathbf{e}_\omega \end{bmatrix} = \begin{bmatrix} \mathbf{i}_s - \hat{\mathbf{i}}_s \\ \boldsymbol{\psi}_r - \hat{\boldsymbol{\psi}}_r \\ \omega_m - \hat{\omega}_m \end{bmatrix}. \tag{11}$$

(2) Linearization of the state estimation error equation around a fixed operating point

The state estimation error equation formulated in the first step is linearized around the fixed operating-point

$$\mathbf{e} = \mathbf{e}_0 + \Delta\mathbf{e}; \quad \hat{\omega}_m = \hat{\omega}_{m0} + \Delta\hat{\omega}_m \tag{12}$$

and the following equation is obtained

$$\frac{d}{dt}\Delta\mathbf{e} = \hat{\mathbf{A}}_0^e \Delta\mathbf{e} + \Delta\hat{\mathbf{A}}_0^e \mathbf{e}. \tag{13}$$

(3) Calculation of eigenvalues of the linearized state matrix (poles of the estimator)

In this step, an analysis of the linearized state matrix is made. The eigenvalues are calculated from the following equation

$$\det(s\mathbf{I} - \hat{\mathbf{A}}_0^e) = 0. \tag{14}$$

(4) Analysis of the position of the real parts of all estimator eigenvalues at fixed operating points

All poles should lie in the left half Gauss plane, therefore the real part of each of them should have a negative sign. A positive sign provides about instability in the certain operating point.

(5) Calculation of the boundaries of instability

The boundaries of instability are determined by comparing the value of the determinant of a linearized state matrix to zero

$$\det \hat{\mathbf{A}}_0^e = 0\,. \tag{15}$$

3.2. STABILITY ANALYSIS OF MRAS^{CC}

The full model of MRAS^{CC} estimator (8) can be rewritten as follows

$$\begin{cases} T_N \dfrac{d}{dt}\hat{\mathbf{i}}_s = \left(-\dfrac{r_1}{l_\sigma} - j\omega_s\right)\hat{\mathbf{i}}_s + \left(\dfrac{k_r}{l_\sigma \tau_r} - j\dfrac{k_r}{l_\sigma}\hat{\omega}_m\right)\hat{\boldsymbol{\psi}}_r + \dfrac{1}{l_\sigma}\mathbf{u}_s + \mathbf{g}_s \mathbf{e}_i, \\ T_N \dfrac{d}{dt}\hat{\boldsymbol{\psi}}_r = r_r k_r \mathbf{i}_s + \left(-\dfrac{1}{\tau_r} - j\left(\omega_s - \hat{\omega}_m\right)\right)\hat{\boldsymbol{\psi}}_r + \mathbf{g}_r \mathbf{e}_i, \\ \dfrac{d}{dt}\hat{\omega}_m = -K_i \varepsilon' - K_p \dfrac{d}{dt}\varepsilon'. \end{cases} \tag{16}$$

The following state matrix is obtained after linearization of the state estimation error equation

$$\hat{\mathbf{A}}_0^e = \begin{bmatrix} -\dfrac{r_1}{l_\sigma} - j\omega_{s0} - \mathbf{g}_s & \dfrac{k_r}{l_\sigma \tau_r} - j\dfrac{k_r}{l_\sigma}\hat{\omega}_{m0} & -j\dfrac{k_r}{l_\sigma}\boldsymbol{\psi}_{r0} \\ -\mathbf{g}_r & -\dfrac{1}{\tau_r} - j(\omega_{s0} - \hat{\omega}_{m0}) & j\boldsymbol{\psi}_{r0} \\ \mathbf{a}_{sO} & \mathbf{a}_{rO} & a_{\omega O} \end{bmatrix} \tag{17}$$

where $\omega_{s0} - \hat{\omega}_{m0} = \hat{\omega}_{r0}$; $\mathbf{a}_{sO} = [a_{51} \quad a_{52}]$; $\mathbf{a}_{rO} = [a_{53} \quad a_{54}]$; $a_{\omega O} = a_{55}$.

Details concerning values of the a_{51}–a_{55} coefficients and the matrix $\Delta\hat{\mathbf{A}}_0^e$ (in (13)) are given in the Appendix. It is also assumed that $\psi_{rx0} = \psi_{ref}$, $\psi_{ry0} = 0$.

A graph of unstable operating points is created by analysing the poles of the estimator according to (14) in the following range

$$\left(\pm\omega_{mn}\ ;\ \pm 2\omega_{r0} \approx \pm 2m_n \xleftarrow{\text{because}} m_L = \frac{\psi_{ref}^2 \omega_{r0}}{r_r}\right).$$

During the above calculations the following assumptions were made: $\mathbf{g}_s = \mathbf{0}$, $\mathbf{g}_r = \mathbf{0}$, $\varphi = 0$, to check the stability region of an original (not modified) estimator [22]. The placement of the unstable estimator eigenvalues is presented in Fig. 5. It should be noted that the estimator is unstable in the regenerating mode in the whole range examined. The two eigenvalues (λ_4 and λ_5) are responsible for these properties.

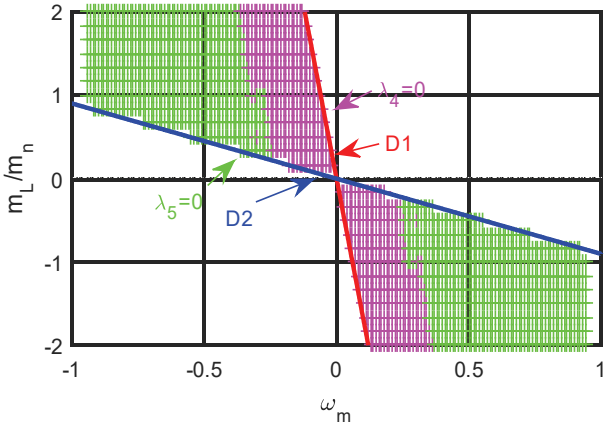

Fig. 5. Unstable eigenvalues of the estimator MRAS^{CC} and straight lines boundaries D1 and D2: $\mathbf{g}_s = \mathbf{0}$, $\mathbf{g}_r = \mathbf{0}$, $\varphi = 0$, $K_p = 0.5$, $K_i = 30$

The next step is to designate the boundaries which limit the range of unstable operating points. Thus, according to (14) the determinant of the linearized system state matrix $\hat{\mathbf{A}}_0^e$ is calculated and its value is compared to zero

$$\det \hat{\mathbf{A}}_0^e = -\frac{K_i \psi_{ref}^2}{l_\sigma^2 l_r} \omega_{s0} (l_r r_s k_r \omega_{r0} + l_r r_r k_r^3 \omega_{r0} + l_\sigma r_r k_r \omega_{s0}) = 0 . \tag{18}$$

The condition (18) will be fulfilled when

$$\omega_{s0} = 0 \quad \text{or} \quad \omega_{s0} = \omega_{m0} \frac{r_s + r_r k_r^2}{r_s + \dfrac{l_\sigma}{\tau_r} + r_r k_r^2} . \tag{19a}$$

The obtained straight lines given by equations (19a) (boundaries of the unstable operating points caused by unstable estimator eigenvalues λ_4 and λ_5) in the plane $\omega_s \leftrightarrow \omega_m$ can be easily recalculated to the plane $m_L \leftrightarrow \omega_m$ and are marked next as lines D1 and D2 in Fig. 5,

$$\begin{cases} m_L = -\dfrac{\psi_{ref}^2}{r_r}\omega_{m0} & \rightarrow \text{D1}, \\ m_L = -\dfrac{\psi_{ref}^2}{r_r}\omega_{m0}\left(\dfrac{\dfrac{l_\sigma}{\tau_r}}{r_s + \dfrac{l_\sigma}{\tau_r} + r_r k_r^2}\right) & \rightarrow \text{D2}. \end{cases} \tag{19b}$$

It should be noted that the coefficient K_p does not affect the unstable range of operating points and the value of the determinant (see (18)).

4. STABILIZATION METHODS FOR THE ESTIMATOR

The stability in regenerating mode of the MRAS^{CC} estimator discussed in this article can be improved by appropriate selection of the gain matrix **G** coefficients (as in (7), (8)) or by shifting the stator current error versus rotor flux vector with the angle ϕ in the adaptation mechanism (according to (9)). Then the position of the border line D2 is changed. The aim of such modification is to obtain unstable operating points only on line D1 so that line D2 must be equal to D1. It follows that the aim is to obtain the following value of the determinant of the linearized system state matrix

$$\det \hat{\mathbf{A}}_0^e = -\alpha\omega_{s0}^2, \tag{20}$$

where α is a positive constant depending on the stabilization method used.

4.1. SELECTION OF THE GAINS MATRIX COEFFICIENTS

In order to select coefficients of the gain matrix **G** the determinant of a linearized state matrix of the estimation error with non-zero values $\mathbf{g}_s \neq \mathbf{0}$, $\mathbf{g}_r \neq \mathbf{0}$ (and $\varphi = 0$) is calculated and takes the following form

$$\det \hat{\mathbf{A}}_0^e = -\frac{K_i \Psi_{ref}^2}{l_\sigma^2 l_r}\omega_{s0} \left(\begin{array}{l} \omega_{s0}(l_r r_s k_r + l_r r_r k_r^3 + l_\sigma r_r k_r + l_\sigma l_r k_r g_{sx}) \\ -\omega_{m0}(l_r r_s k_r + l_r r_r k_r^3 + l_r k_r^3 g_{rx} + l_\sigma l_r k_r g_{sx}) + l_\sigma r_r k_r g_{sy} + r_r k_r^2 g_{ry} \end{array}\right). \tag{21}$$

Thus the gain values which satisfy the condition given by (20) are obtained

$$\begin{cases} g_{sx} = k\dfrac{r_r}{l_r}, & g_{sy} = k\omega_{m0}, \\ g_{rx} = -\dfrac{r_s}{k_r^2}, & g_{ry} = l_r k_r \omega_{m0}, \end{cases} \tag{22}$$

where $k > 0$.

It should be noted that g_{sy} and g_{ry} depend on the measured value of the angular velocity. In sensorless systems the actual speed of the induction motor is unknown. Replacing it with the estimated value of the speed will not give evidence to global stability of the estimator. Therefore, the following approximation resulting from the D1 equation is used

$$\omega_{m0} \sim -\omega_{r0}\,. \tag{23}$$

With the above approximation the following gain coefficients are obtained

$$\begin{cases} g_{sx} = k\dfrac{r_r}{l_r}, & g_{sy} = -k\omega_{r0}, \\ g_{rx} = -\dfrac{r_s}{k_r^2}, & g_{ry} = -l_r k_r \omega_{r0}\,. \end{cases} \tag{24}$$

In Fig. 6, the resulting placement of the modified estimator eigenvalues is presented for accurate and approximate values of the gain matrix coefficients (22) and (24), respectively.

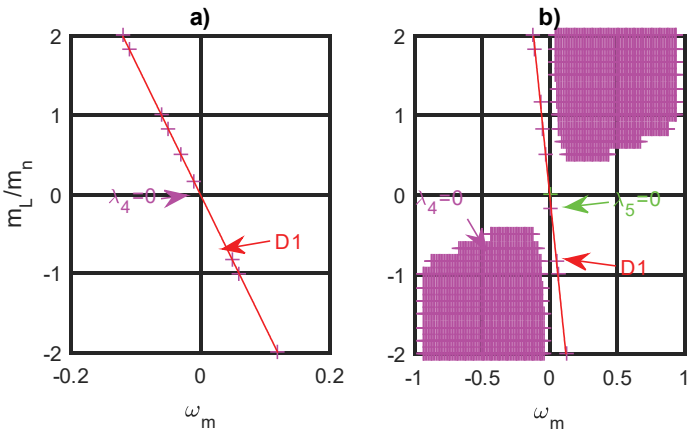

Fig. 6. Unstable operating points when $\varphi = 0$, $K_p = 0.5$, $K_i = 30$: (a) $\mathbf{g}_s$ and $\mathbf{g}_r$ – equation (22), (b) $\mathbf{g}_s$ and $\mathbf{g}_r$ – equation (24)

Appropriate selection of the gain matrix **G** coefficients for the estimator MRAS^{CC} allows expected properties to be achieved. The range of instability becomes just a straight line D1 (Fig. 6a). Unfortunately, approximation (24) leads to the appearance of unstable operating points in motoring mode (Fig. 6b). It means that the gain matrix coefficients should become zero under the transition from the regenerating mode to motoring mode.

4.2. SELECTION OF THE SHIFT ANGLE FOR MRAS^{CC}

Another way to improve stability of the estimator is appropriate selection of the shift angle between the stator current error and the rotor flux. In order to calculate this value, the determinant of the linearized state matrix of estimation error for $\varphi \neq 0$ and $\mathbf{g}_s = \mathbf{0}$, $\mathbf{g}_r = \mathbf{0}$ is presented

$$\det \hat{\mathbf{A}}_0^e = -\frac{K_i \Psi_{ref}^2}{l_\sigma^2 l_r} \omega_{s0} \left(\begin{array}{l} \omega_{s0}(\cos\phi(l_r r_s k_r + l_r r_r k_r^3 + l_\sigma r_r k_r) - \sin\phi(l_\sigma l_r k_r \omega_{r0})) \\ -l_r r_s k_r \omega_{m0} \cos\phi - l_r r_r k_r^3 \omega_{m0} \cos\phi + r_r r_s k_r \sin\phi + r_r^2 k_r^3 \sin\phi \end{array} \right). \tag{25}$$

Taking into account (20), the following value of the shift angle is obtained

$$\varphi = \tan^{-1}\left(\frac{l_r}{r_r}\omega_{m0}\right). \tag{26}$$

As for the gain matrix, the approximation (23) is used

$$\varphi = -\tan^{-1}\left(\frac{l_r}{r_r}\omega_{r0}\right). \tag{27}$$

As follows from Fig. 7a, the shift angle is well chosen, but only in the low speed range. Unfortunately, with increasing speed unstable operating points appear. The instability in regenerating mode disappears after increase of the coefficients in the adaptation algorithm (K_p and K_i), which is shown in Fig. 7b.

The use of approximation (27) allows the unstable operating points to be completely reduced (even for smaller values coefficient K_p) (see Fig. 8). Of course, the unstable eigenvalues appear only on the straight line D1 ($\omega_{s0} = 0$). In the case of transition from the regenerating mode to motoring mode the value of the shift angle should be changed to zero; otherwise the estimator may be unstable in the motoring mode.

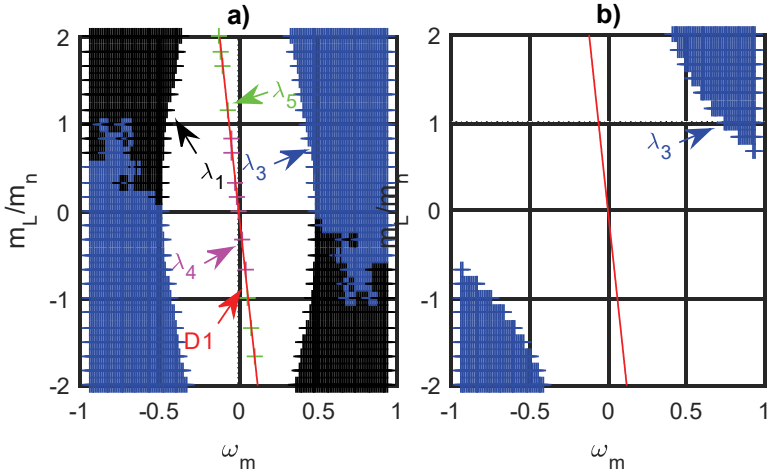

Fig. 7. Unstable operating points when $\mathbf{g_s} = 0$, $\mathbf{g_r} = 0$, φ – equation (25): (a) $K_p = 0.5$, $K_i = 30$, (b) $K_p = 100$, $K_i = 1000$

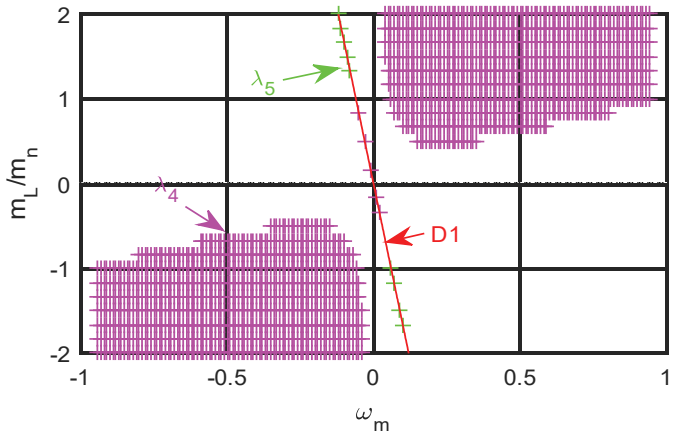

Fig. 8. Unstable operating points when $\mathbf{g_s} = 0$, $\mathbf{g_r} = 0$, φ – equation (27), $K_p = 0.5$, $K_i = 30$

5. SIMULATION TESTS OF THE ESTIMATOR IN DRFOC STRUCTURE

Under the simulation tests the induction motor drive was controlled using the Direct Rotor flux Field-Oriented Control (DRFOC), the structure of which is shown in Fig. 9. Simulation tests were done in the regenerating mode of the drive system and the MRAS^{CC} estimator behaviour was analysed for the following speed reference values $\omega_m = \{\pm 0.1 \quad \pm 0.3 \quad \pm 0.5 \quad \pm 0.7 \quad \pm 0.9\}\omega_{mn}$. When the motor speed had reached

the assumed reference value, the load torque was applied. The load torque was growing for 20 s from zero to twice the nominal value.

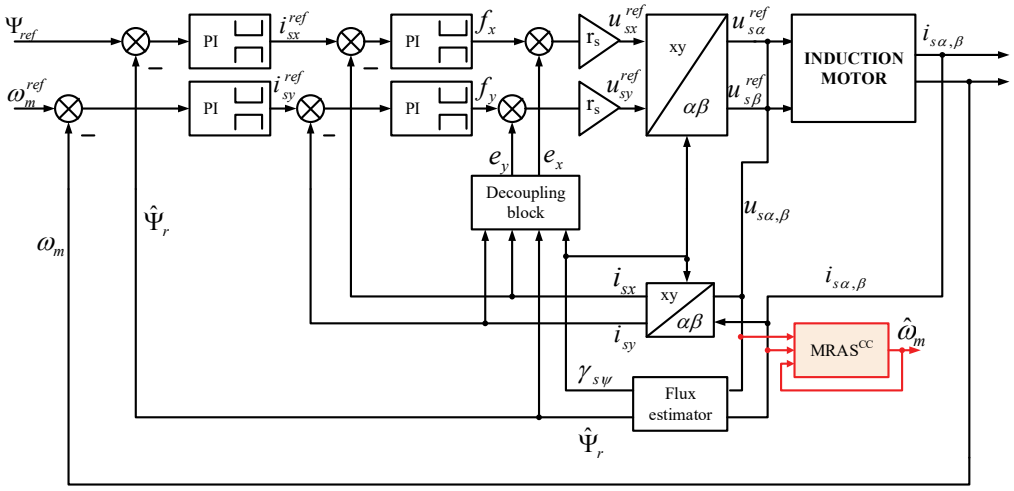

Fig. 9. The DRFOC control structure used in the simulation tests

Figure 10 shows an example of simulation results. It illustrates the behaviour of the estimator for the reference speed $\omega_m = 0.3\omega_{mn}$ and slowly changing regenerative load torque in the range $(0 \div -2)m_n$. It is seen that for certain value of the load torque the estimator loses the stability. Similar simulation tests have been realised for other above-mentioned values of reference speed and results are plotted in the plane $m_L \leftrightarrow \omega_m$ in Figs. 11–13.

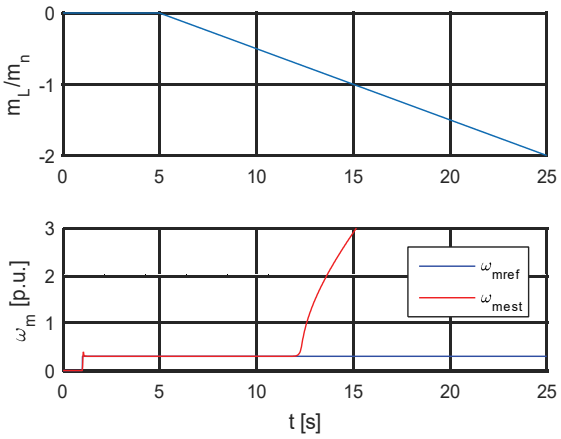

Fig. 10. An example of the load torque, the reference speed and estimated speed

In the following figures the results confirming the theoretical analysis shown in the previous sections are presented. Traces in Fig. 11 confirm theoretically defined unstable regions of the classical MRAS^{CC} [22] in the regenerating mode. For each of the test speed reference values, MRAS^{CC} loses the stability inside the appointed region. Therefore, the estimator should be stabilized by appropriate selection of the gain matrix coefficients or the shift angle value. The behaviour of the estimator for both stabilization methods is shown in Fig. 12 and Fig. 13, respectively.

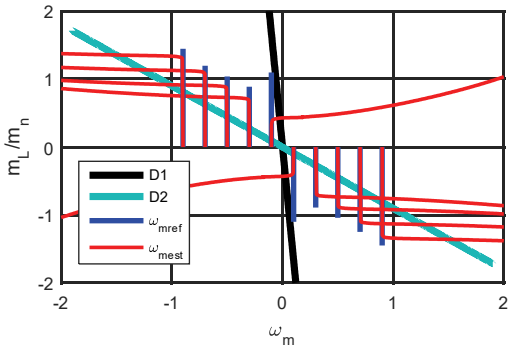

Fig. 11. Unstable operating points for classical MRAS^{CC} with $\mathbf{g}_s = \mathbf{0}$, $\mathbf{g}_r = \mathbf{0}$, $\varphi = 0$, $K_p = 0.5$, $Ki = 30$

From Fig. 12a it results that in the case of knowledge of the actual induction motor speed, the estimator with gain matrix selected according to (22) is stable in the full range of speed. The use of approximation of the motor speed by slip frequency (24) leads to unstable operating points in the motoring mode (Fig. 12b). This confirms that the gain matrix should be adjusted to zero under the transition from regenerating to motoring mode.

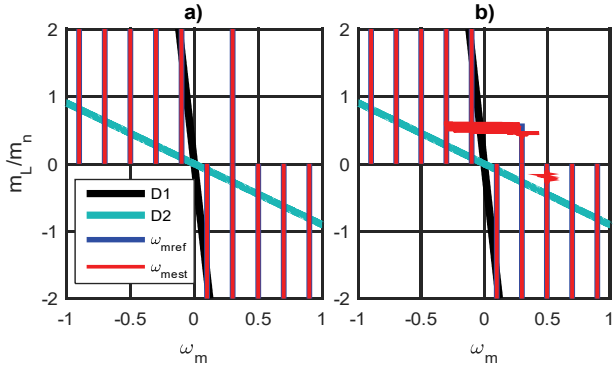

Fig. 12. Unstable operating points of the modified MRAS^{CC} with $\varphi = 0$, $K_p = 0.5$, $K_i = 30$: (a) matrix **G** according to (22); (b) matrix **G** according to (24)

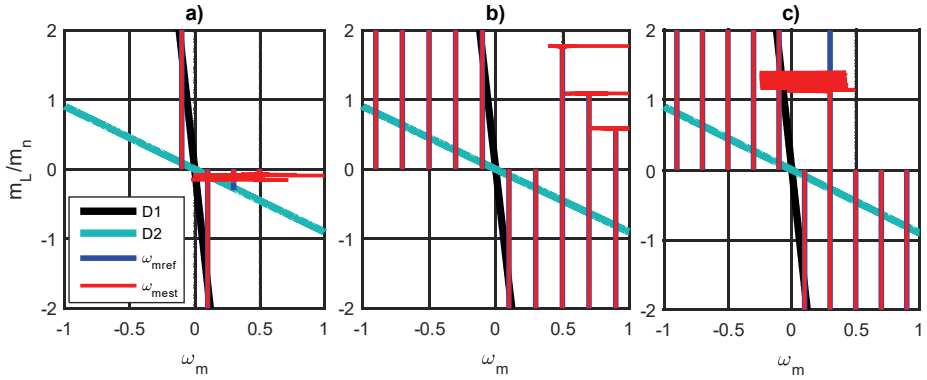

Fig. 13. Unstable operating points of the modified MRAS^{CC}: (a) angle φ according to (26), $K_p = 0.5$, $K_i = 30$; (b) angle φ according to (26), $K_p = 100$, $K_i = 1000$; (c) angle φ according to (27), $K_p = 0.5$, $K_i = 30$

Figures 13a, b show the effect of increasing the coefficients in the adaptation mechanism to improve stability, when equation (26) is used for the calculation of angle φ. The increase of K_p and K_i reduces the range of unstable operating points in motoring mode. However, if equation (27) is applied to angle calculation, then similarly as in the case of the gain matrix (24), the value of the shift angle should be switched to zero under transition from the regenerating mode to motoring mode. If the angle is not switched on, then the unstable operating points appear in the motoring mode (Fig. 13c).

6. CONCLUSION

The modified version of the speed estimator MRAS^{CC}, with two stabilization mechanisms proposed in the literature for the Adaptive Full Order Observer [8]–[11] to improve the estimator stability in the regenerating mode, was analysed in this paper. The range of unstable operating points which appear in the regenerating mode was determined by the stability analysis. The results obtained are similar to those shown in [24], but the present analyses confirmed by simulation results are more detailed.

Analysis of the determinant of the state matrix of the linearized estimation error equation makes it possible to determine the appropriate elements (coefficients of the gains matrix or shift angle between the stator current error and the rotor flux vectors) stabilizing the MRAS^{CC} estimator operation in the regenerating mode and to reduce the range of unstable operation points to the straight line D1 ($\omega_{s0} = 0$). In this article, both gain matrix and shift angle choice has been proposed and analysed. From the extended simulation tests it results that the gain matrix elements or shifting angle should be set to zero under the transition from the regenerating to monitoring mode and vice versa.

Simulation tests confirm the theoretically determined range of the MRAS^{CC} instability in regenerating mode and the conditions when this estimator behaves stable in this range.

APPENDIX

Coefficients a_{51}–a_{55} are given as follows

$$\begin{aligned}
a_{51} &= -\psi_{ref}\sin\phi\left[K_i - K_p\left(\frac{r_1}{l_\sigma}+g_{sx}\right)\right] - K_p\psi_{ref}(\omega_{s0}+g_{sy})\cos\phi,\\
a_{52} &= \psi_{ref}\cos\phi\left[K_i - K_p\left(\frac{r_1}{l_\sigma}+g_{sx}\right)\right] - K_p\psi_{ref}(\omega_{s0}+g_{sy})\sin\phi,\\
a_{53} &= -\frac{K_p\psi_{ref}k_r\,\omega_{m0}\cos\phi}{l_\sigma} - \frac{K_p\psi_{ref}k_r\sin\phi}{\tau_r l_\sigma},\\
a_{54} &= \frac{K_p\psi_{ref}k_r\cos\phi}{\tau_r l_\sigma} - \frac{K_p\psi_{ref}k_r\,\omega_{m0}\sin\phi}{l_\sigma},\\
a_{55} &= -\frac{K_p\psi_{ref}^2 k_r\cos\phi}{l_\sigma}.
\end{aligned} \tag{28}$$

Matrix $\Delta\hat{\mathbf{A}}_0^e$ has the following form

$$\Delta\hat{\mathbf{A}}_0^e = \begin{bmatrix} -j\Delta\omega_s & -j\dfrac{k_r}{l_\sigma}\Delta\omega_m & 0\\ 0 & -j\Delta\omega_s + j\Delta\omega_m & 0\\ 0 & 0 & 0 \end{bmatrix}. \tag{29}$$

Table 1. Parameters of the induction motor

Parameter	Value [physical unit]	Value [per unit]
Nominal power	P_N = 1500 [W]	p_n = 0.6211
Nominal torque	M_N=10.1588 [N]	m_n = 0.6608
Nominal voltage	U_N = 230 [V]	u_n = 0.7071
Nominal current	I_N = 1.5 [A]	i_n = 0.7071
Nominal motor speed	n_N = 1440 [obr/min]	ω_{mn} = 0.94
Magnetizing inductance	L_m = 278.5 [mH]	l_m = 1.3314
Stator/rotor inductance	L_s = L_r = 295.8 [mH]	l_r = l_s =1.4141
Stator resistance	R_s = 5.3073 [Ω]	r_s = 0.0808
Rotor resistance	R_r = 4.8430 [Ω]	r_r = 0.0737
Flux	Ψ_r = 0.9328 [Wb]	ψ_r = 0.9009
Frequency	f_{sN} = 50 [Hz]	–
The number of pole pairs	p_b = 2	–
Moment of interia	J = 0.0193 [kgm^2]	–

REFERENCES

[1] KAŹMIERKOWSKI M.P., BLAABJERG F., KRISHNAN R., *Control in Power Electronic – Selected Problems*, Academic Press, USA, 2002.
[2] HOLTZ J., *Sensorless Control of Induction Machines – With or Without Signal Injection?*, IEEE Trans. Industrial Electronics, 2006, 53 (1), 7–30.
[3] ORŁOWSKA-KOWALSKA T., *Sensorless induction motor drives*, Oficyna Wydawnicza PWr, Wrocław 2003, (in Polish).
[4] UTKIN V., YAN Z., *Sliding mode observers for electronic machines – an overview*, Proc. of the 28th Annual Conf. of the Industrial Electronics Society IECON 2002, Sevilla 2002, 3, 2, 1842–1847.
[5] BOLDEA I., LASCU C., BLAABJERG F., *A class of speed-sensorless sliding-mode observers for high-performance induction motor drives*, IEEE Trans. Industrial Electronics, 2009, 56, 9, 3394–3403.
[6] KUBOTA H., MATSUSE K., NAKANO T., *DSP-based speed adaptive flux observer of induction motor.* IEEE Trans. Industry Appl., 1993, 29, 2, 344–348.
[7] BOUHENNA A., MANSOUR A., CHENAFA M., BELAIDI A., *Feedback Gain Design Method for the Full-Order Flux Observer in Sensorless Control of Induction Motor*, International Journal of Computers Communications and Control, 2008, 3, 2, 135–148.
[8] BOUHENNA A., CHAIGNE C., BENSIALI N., ETIEN E., CHAMPENOIS G., *Design of speed adaptation law in sensorless control of induction motor in regenerating mode*, Simulation Modelling Practice and Theory, August 2007, 15, 7, 847–863.
[9] ETIEN E., CHAIGNE C., BENSIALI N., *On the Stability of Full Adaptive Observer for Induction Motor in Regenerating Mode*, IEEE Trans. Ind. Electronics, 2010, 57, 5, 1599–1608.
[10] HINKKANEN M., LUOMI J., *Stabilization of regenerating-mode operation in sensorless induction motor drives by full-order flux observer design*, IEEE Trans. Ind. Electronics, 2004, 51, 6, 1318–1328.
[11] HARNEFORS L., HINKKANEN M., *Complete stability of reduced-order and full-order observers for sensorless IM drives*, IEEE Trans. Ind. Electronics, 2008, 55, 30, 1319–1329.
[12] KUBOTA H., SATO I., TAMURA Y. et al., *Regenerating-mode low-speed operation of sensorless induction motor drive with adaptive observer*, IEEE Trans. Industry Appl., 2002, 38, 4, 1081–1086.
[13] SUNWANKAWIN S., SANGWONGWANICH S., *Design strategy of an adaptive full-order observer for speed-sensorless induction motor drives – Tracking performance and stabilization*, IEEE Trans. Industrial Electronics, 2006, 53, 1, 96–119.
[14] ABU-RUB H., OIKONOMOU N., *Sensorless observer system for induction motor control*, Proc. of the IEEE Power Electronics Specialists Conference, Rodos 2008, 30–36.
[15] ORŁOWSKA-KOWALSKA T., DYBKOWSKI M., TARCHAŁA G., *Analysis of the chosen estimation methods in the induction motor drives* – part I – *mathematical models*, Scientific Papers of the Institute of Electrical Machines, Drives and Measurements, Studies and Research, 2010, 30, 151–161.
[16] DYBKOWSKI M., TARCHAŁA G., ORŁOWSKA-KOWALSKA T., *Analysis of the chosen estimation methods in the induction motor drives* – part II – *research tests*, Scientific Papers of the Institute of Electrical Machines, Drives and Measurements, Studies and Research, 2010, 30, 162–175.
[17] SCHAUDER C., *Adaptive speed identification for vector control of induction motors without rotational transducers*, IEEE Trans. on Industry Applications, Sept./Oct. 1992, 28, 5, 1054–1061.
[18] TAMAI S. et al., *Speed sensorless vector control of induction motor with model reference adaptive system*, Proc. of IEEE/IAS, 1987, 189–195.
[19] PENG F.Z., FUKAO T., *Robust speed identification for speed-sensorless vector control of induction motors*, IEEE Trans. on Industry Applications, 1994, 30, 5, 1234–1240.

[20] PENG F.Z., FUKAO T., LAI J.S., *Low-speed performance of robust speed identification using instantaneous reactive power for tacholess vector control of induction motors*, Proc. IEEE Industry Applications Society Annual Meetings, 1994, 1, 509–514.

[21] SOBCZUK D.L., *Application of ANN for control of PWM inverter fed induction motor drives*, Ph.D. dissertation, Warsaw Univ. Technol, Warsaw, Poland, 1999.

[22] ORŁOWSKA-KOWALSKA T., DYBKOWSKI M., *Stator current-based MRAS speed estimator for wide range speed-sensorless induction motor drive*, IEEE Trans. Ind. Electronics, 2010, 57, 4, 1296–1308.

[23] ORŁOWSKA-KOWALSKA T., TARCHAŁA G., *Unified approach to the sliding-mode control and state estimation – application to the induction motor drive*, Bulletin of the Polish Academy of Sciences. Technical Sciences, 2013, 61, 4, 837–846.

[24] VONKOMER J., ZALMAN M., *On the stability of current based MRAS*, Proc. of the 39th Annual Conf. of the Industrial Electronics Society IECON 2013, Nov. 2013, 3018–3023.